Article

J. Mex. Chem. Soc. **2024**, *68*(3)
Regular Issue

ISSN-e 2594-0317

Experimental and Statistical Investigation of a Novel Green Inhibitor *Ferula Lutea* as Potential Corrosion Inhibiting Carbon Steel in an Acidic Medium

Wafia Boukhedena[1,3,*], Samir Deghboudj[2,3], Merzoug Benahmed[4], Hocine Laouer[5]

[1]Department of Science Materials, Larbi Tebessi University, Constantine Road, 12002 Tebessa, Algeria.
[2]Department of Mechanics, Larbi Tebessi University, Constantine Road, 12002, Tebessa, Algeria.
[3]Mines Laboratory, Larbi Tebessi University, Constantine Road, 12002, Tebessa, Algeria.
[4]Laboratory of Bioactive Molecules and Applications, Constantine Road, 12002, Tebessa, Algeria.
[5]Laboratory for the Valorization of Natural Biological Resources, Ferhat Abbas University, Setif, 19000, Algeria.

***Corresponding author:** Wafia Boukhedena, email: wafia.boukhedena@univ-tebessa.dz

Received October 25th, 2022; Accepted June 6th, 2023.

DOI: http://dx.doi.org/10.29356/jmcs.v68i3.1891

Abstract. Carbon steel corrosion inhibition in the presence and absence of *Ferula lutea* butanolic extract (EBFL) as a corrosion inhibitor was investigated. This study focuses on the optimization of three main parameters: inhibitor concentration, immersion time, and temperature, on the corrosion inhibition of X2C30 carbon steel by EBFL based on the weight loss method. A composite-centered design (CCD) of response surface methodology (RSM) was employed to design the experiment utilizing Design Expert software in to assess the experimental factors that influence the process. Both the corrosion rate and the inhibition efficiency were modeled using logarithmic quadratic equations. The achieved correlation between the predicted and experimental values reveals the accuracy of the proposed models. This investigation proved that (RSM) is a useful tool to predict the optimal operating parameters of the examined inhibitor to mitigate carbon steel corrosion. Gravimetric and electrochemical measurements have indicated that extract (EBFL) exhibits corrosion inhibition properties of X2C30 carbon steel in 1 M hydrochloric acid medium.
Keywords: Corrosion; carbon steel; *Ferula lutea*; weight loss measurements; surface response methodology.

Resumen. Se investigó la inhibición de la corrosión del acero al carbono en presencia y ausencia del extracto butanólico de *Ferula lutea* (EBFL) como inhibidor de la corrosión. Este estudio se centra en la optimización de tres parámetros principales: la concentración del inhibidor, el tiempo de inmersión y la temperatura, sobre la inhibición de la corrosión del acero al carbono X2C30 por el EBFL basándose en el método de la pérdida de peso. Se empleó un diseño centrado en el compuesto (CCD) de la metodología de superficie de respuesta (RSM) para diseñar el experimento utilizando el software Design Expert en para evaluar los factores experimentales que influyen en el proceso. Tanto la velocidad de corrosión como la eficiencia de inhibición se modelaron mediante ecuaciones cuadráticas logarítmicas. La correlación alcanzada entre los valores predichos y los experimentales revela la precisión de los modelos propuestos. Esta investigación demostró que (RSM) es una herramienta útil para predecir los parámetros operativos óptimos del inhibidor examinado para mitigar la corrosión del acero al carbono. Las mediciones gravimétricas y electroquímicas han indicado que el extracto (EBFL) presenta propiedades de inhibición de la corrosión del acero al carbono X2C30 en medio ácido clorhídrico 1 M.
Palabras clave: Corrosión; acero al carbono; *Ferula lutea*; medidas de pérdida de peso; metodología de respuesta superficial.

J. Mex. Chem. Soc. **2024**, *68*(3)
Regular Issue

ISSN-e 2594-0317

Introduction

Steel and its alloys are widely used in the construction of tanks, pipes and oil refining equipment [1,2]. These installations are highly vulnerable to corrosion and have a low resistance to aggressiveness in the presence of acid solutions, which are often used to remove unwanted scale and rust in many industrial processes. The most widely commercialized and used acid is hydrochloric acid (HCl). To effectively control corrosion of carbon steel there are several methods, however, corrosion inhibitors remain among the most effective and practical methods [3-6].

Inhibitors are being used to control steel dissolution and reduce acid consumption [6,7]. Currently, research on inhibitors includes a variety of activities ranging from protective mechanisms to the monitoring of industrial systems in which inhibitors are utilized, to the discovery and synthesis of new compounds, to the assessment of competitively traded products [8]. Corrosion inhibitors are organic and inorganic substances, which are added to the corrosive environment in an attempt to reduce or eliminate corrosion. These substances are adsorbed to the metal surface and change the structure of the electrical double layer. The adsorption process depends mainly on the molecular structure. However, the use of some organic and inorganic chemical inhibitors is limited because their synthetically produced compounds are very high in cost, their biodegradability is limited and they are toxic, harmful, and dangerous to humans and the environment [9,10]. The most recent research in the domain are focused on the corrosion-inhibiting properties of natural plant extracts [11,12]. These represent extremely rich sources of natural chemical compounds that are eco-friendly and not harmful, cheap, available, and abundant, renewable, and can be extracted by simple processes and techniques.

A substantial number of reports, reviews, and books have been devoted to the use of green plant-based corrosion inhibitors for metals in acidic mediums. It has been stated that plant extracts have excellent inhibiting abilities, with low or no negative impact on the environment. Several types of research are available justifying the suitability of the plant-based inhibitor. Among the various inhibitors of plant origin studied, we mention particularly those dedicated to the protection of metals against corrosion in acidic environments. Valek and Martinez [13] investigated the inhibition of the corrosion of the copper in sulfuric acid 0.5 M by leaf extract of *Azadirachta indica*. The methods used were intensity-potential curves and weight loss. Azadirachta indica revealed an efficacy of 86.4 %. The effect of *Punica granatum* extract and its main constituents on the inhibition of mild steel in 2 M HCl and 1 M H_2SO_4 solutions was examined by M. Behpour et al. [14] using weight loss, potentiodynamic polarization and electrochemical impedance spectroscopy (EIS) for various concentrations of the extract. *Azadirachta indica* exhibited an inhibitory efficiency of 95.8 % in HCl solution and 94.2 % in H_2SO_4 solution. N. Soltani *et al.* [15] studied the influence of *Silybum marianum* leaf extract as a corrosion inhibitor of 304 stainless steel in 1.0 M HCl solution. The highest extract concentration, 1.0 g/L, leads to a rise in inhibitory efficiency that reaches 96 %. In recent research, the inhibitory effect of *Laurus nobilis* leaf extract for carbon steel in 1M HCl acid medium was examined [16]. The achieved findings indicated a maximum protection of 92 %, which was obtained after 2.5 h at a concentration of 400 ppm of the extract.

In general, for any material, there is a suitable family of inhibitors to provide satisfactory protection against corrosion. Extracts of certain plants such as *Portulaca grandiflora* [17], *Ficus tikoua leaves* [18], *Neolamarckia cadamba barks* [19], *Ephedra Major* [20], *Thapsia villosa* [21], *Arthrospira platensis* [22], *Sansevieria trifasciata* [23], *Orange peel* [24], have been reported to inhibit corrosion of metals in acid solutions.

Analytical chemistry is increasingly using response surface methodology (RSM) as a tool for optimization. It comprises a group of statistical and mathematical methods based on fitting empirical models to experimental data gathered following the experimental design. To achieve this goal, the studied system is described using linear or square polynomial functions, which are then used to investigate (by modeling) the experimental conditions until its optimization [25-30].

The present work is part of the experimental investigations on the inhibition of corrosion of metal surfaces by the use of green inhibitors. It is in this regard that we examined the corrosion inhibition of a X2C30 carbon steel by the butanolic extract of the plant *Ferula lutea* denominated (EBFL) in a 1 M hydrochloric acid medium. We applied electrochemical and gravimetric techniques to determine the efficiency of the inhibitor, its mode of acting as well as several corrosion parameters. The values of the most significant operational parameters have been optimized using the response surface methodology (RSM) based on composite-centered design (CCP) to enhance the associated responses. The two responses examined were: inhibitory efficiency and corrosion rate. The building

J. Mex. Chem. Soc. **2024**, *68*(3)
Regular Issue

ISSN-e 2594-0317

of the experimental design, the statistical analysis, and the graphical representation of the model as well as the optimization study of the factors that influence these responses were carried out using the design-Expert software.

Materials and methods

Samples preparation

The material used as the working electrode is a carbon steel of quality X2C30, having the following chemical composition (in % by weight): C (0.35); Si (0.4); Mn (0.8); P (0.035); S (0.035) and Fe remainder. Weight loss measurements were conducted on prepared 1×1×1 cm cubes abraded successively with different grades of emery paper (320, 400, 500, 800, 1000, 1200, and 2000), washed with distilled water, cleaned with acetone, and dried at room temperature before being utilized in the experiments.

Preparation of HCl solution

The corrosive medium is a 1 M hydrochloric acid solution, obtained by diluting the commercial concentrated acid of HCl 37 % (Merck) with distilled water. The tests were carried out in this solution without and with the addition of different concentrations (200,500 and 800 ppm) of the extract: n-Butanol of the plant *Ferula lutea* (EBFL).

Solid-liquid extraction

The plant was collected during its flowering period in May in the area of mountain Babor in the province of Setif in eastern Algeria. Solid-liquid extraction employed in this work is a technique, which consists in letting the plant material (cut in small pieces) stay in the water/methanol mixture (aqueous methanol) to extract the active principles (phenolic compounds and flavonoids). The protocol for the n-butanolic extract of *Ferula lutea* was carried out according to the literature reports [20,31,32].

Weight loss measurements

This method is relatively easy and does not require any important equipment. It consists of exposing surface samples (S) in HCl 1M medium in the absence and presence of different concentrations of the inhibitor (EBFL) maintained at constant temperature for a well-defined time (t) and measuring the mass difference (ΔW) of the samples before (W_i) and after (W_f) for each test. (1): The loss in weight, corrosion rate, and inhibitor efficiency were established according to the following relationship:

$$CR = \frac{\Delta W}{S.t} \tag{1}$$

The inhibition efficiency (IE_W %) can be calculated using Equation (2):

$$IE_W\,\% = \left(\frac{CR_0 - CR_i}{CR_0}\right) \times 100 \tag{2}$$

where, CR_0 and CR_i are the corrosion rates in the absence and presence of various concentrations of inhibitor respectively. The corrosion rate (CR) and the inhibition efficiency (IE_w%) are very useful to discuss the adsorption characteristics and thermodynamic parameters that were calculated.

Response surface methodology

An experimental design is a statistical method to control a multi-parameter (factor) problem by following a pre-conceived program of different experiments to be performed. Its purpose is to minimize the number of experiments in order to achieve accurate results that reflect the real variation of the studied phenomenon concerning its different attributes [28,29,33]. A constrained calculation interval is one of the characteristics of this experimental design. The levels utilized, indicated by the values (-1) and (+1), represent the minimum and maximum level values allocated to the components that are centered around a middle value,

J. Mex. Chem. Soc. **2024**, *68*(3)
Regular Issue

ISSN-e 2594-0317

respectively (0). Several parameters influence corrosion inhibition such as inhibitor concentration, immersion time, and temperature. In this work, the responses retained are inhibitory efficiency (EI_W %) and corrosion rate (CR). Composite Centered Design (CCD) based Response Surface Methodology (RSM) was used to investigate and statistically analyze the effect of (EBFL) on corrosion inhibition of carbon steel in 1M HCl acid medium. These modeling methods allow for mathematical models involving different parameters that affect the inhibition efficiency and the corrosion rate. All the planned experiments as well as the statistical analysis of the results were done with Design-Expert, which is a specialized software for the planning and analysis of experiments. Table 1 depicts the various levels and factors that were further into the design of this experiment.

In this work, a fitting analysis is recommended using a model comprising a logarithmic polynomial interaction effects equation. The most common second-order polynomial equation for generating the relevant model terms and fitting the experimental data is formulated as follows:

$$ln(Y) = a_0 + \sum_{i=1}^{k} a_i X_i + \sum_{i=1}^{k} a_{ij} X_i^2 + \sum_{i} \sum_{i=1}^{k} a_{ij} X_i X_j + \varepsilon_i \quad (3)$$

where Y represents the predicted response, i.e., inhibition efficiency (IE_w%) and corrosion rate (CR), a_0, the constant parameter, X_i and X_j the variables, a_i, the i^{th} linear coefficient of the input factor X_i, a_{ii}, the i^{th} quadratic coefficient of the input factors X_i, a_{ij}, the different interaction coefficients between the input factors X_i and X_j (i=1-3, j=1-3), and ε_i, the model error [34]. As an alternative to performing a test campaign involving 27 experiments for the inhibition efficiency and another 27 for the corrosion rate test, this number can be minimized to only 17 for each of these two trials, by selecting and applying an experimental design with RSM and CCD Design and using the Design expert software.

Table 1. Factor levels of the independent variables of the central composite design

Factors	Symbols variables	Min level (-1)	Medium level	Max level (+1)
Concentration (ppm)	A	200	500	800
Temperature (°C)	B	20	35	50
Immersion time (h)	C	1	2	3

Scanning electron microscopy (SEM)

The samples for surface morphological examinations were immersed in a 1 M HCl solution containing the optimal concentration found of the inhibitor (800 ppm) for 3 hours at 20 °C. Then they were removed, washed quickly with distilled water, and dried. The analyses were performed using a scanning electron microscope; model JEOL JSM-6360 LV.

Results and discussion

Weight loss measurements

As depicted in Table, the achieved results of the weight loss tests show that the inhibition efficiency EI_W (%) increases while the corrosion rate decreases with the increase of the inhibitor concentration (EBFL). The inhibition efficiency reaches a maximum value of 87.44 % corresponding to the critical concentration (800 ppm), the immersion time (3 hours), and the lowest temperature (20 °C). This maximum inhibition efficiency is reached when the inhibitor concentration and immersion time have their maximum values. This behavior can be attributed to strong adsorption of the inhibitor on the surface of the carbon steel (X2C30) [35-38]. On the other hand, the lowest inhibition efficiency of 20.61 % is observed when the inhibitor concentration and immersion time are at the lowest level, and the temperature reaches its highest values, i.e. 200 ppm and 1h, respectively.

J. Mex. Chem. Soc. **2024**, *68*(3)
Regular Issue

ISSN-e 2594-0317

Table 2. Central composite matrix of factors A, B, and C and the experimental values of responses Y_1 and Y_2, obtained by weight loss measurements.

Run	**Factor1(A)**	**Factor 2 (B)**	**Factor 3 (C)**	**Response1 (Y_1)**	**Response2 (Y_2)**
N°	**Conc (ppm)**	**Temp (°C)**	**Time (h)**	**IE$_W$ (%)**	**CR (mg/cm².h)**
1	800	20	1	86.88	0.0316
2	500	35	3	56.57	0.1412
3	200	20	1	32.36	0.1785
4*	500	35	2	47.72	0.1523
5	200	50	3	29.64	1.3471
6	500	35	1	42.40	0.1492
7*	500	35	2	47.72	0.1523
8	800	35	2	67.77	0.0939
9*	500	35	2	47.72	0.1523
10	200	35	2	25.71	0.2163
11	800	50	1	62.01	0.5353
12	500	20	2	57.59	0.0636
13	800	20	3	87.44	0.0223
14	200	20	3	37.33	0.1113
15	500	50	2	40.82	0.8913
16	800	50	3	71.90	0.5380
17	200	50	1	20.61	1.1186

*Three points in the center of the model.

ANOVA and regression models

The analysis of variance (ANOVA) is a statistical test (Fisher-Snedecor test) that enables users to analyze the variances of the values generated by the model and those of the residuals. The software suggested the logarithmic quadratic model used (equations 4 and 5), for both responses (inhibitory efficiency and corrosion rate). The significance of the model, each factor, and the interactions are checked using a Fisher's test (F). The more F is greater, the less probability (Prob>F) is, and the more significant the related model and the main coefficients are. If the value of (Prob>F) is lower than 0.05, then the model is significant at a 95 % confidence level [39]. Values between 0.05 and 0.10 indicate that the model terms are significant at 90 % and values higher than 0.10 denote that the model terms are not significant [40,41].

In this study, we have implemented a central composite design, according to which a test campaign consisting of a set of 17 experiments has been elaborated, with three points corresponding to the center of the model. The trials were numbered from 1 to 17. Table 2 represents the planning matrix giving the different combinations of the basic factors: EBFL inhibitor concentration, temperature, and immersion time. The results

J. Mex. Chem. Soc. **2024**, *68*(3)
Regular Issue

ISSN-e 2594-0317

derived from the experimental trials on the samples were used to fit mathematical models that represent the responses of inhibitory efficiency (Y_1) and corrosion rate (Y_2) as a function of the independent variables A, B, and C: inhibitor concentration, temperature, and immersion respectively. The initial analyses of variance for the two responses are provided in Tables 3 and 4, showing the sum of squares and the mean square for every parameter, where the p-value and F-value are set as the ratio of the mean square effect respectively, and the mean square error. Before excluding insignificant terms, the predictive models are expressed in terms of the variables in the following equations:

$$Ln(Y_1) = 3.85 + 0.48A - 0.16B + 0.095C + 0.019AB - 0.044AC + 0.045BC - 0.1A^2 + 0.049B^2 + 0.059C^2 \quad (4)$$

and:

$$Ln(Y_2) = -1.89 - 0.58A + 1.3B - 0.069C + 0.21AB - 7.132\times10^{-3}AC + 0.13BC - 0.047A^2 + 0.47B^2 + 0.029C^2 \quad (5)$$

Table 3. Initial ANOVA results and statistical parameters for response Y_1.

Source	**Sum of squares**	**df**	**Mean square**	**F-Value**	**p-Value Prob>F**	**Observation**
Model	2.70	9	0.30	212.39	< 0.0001	**Significant**
A-Conc	2.30	1	2.30	1628.83	< 0.0001	
B-Temp	0.24	1	0.24	172.07	< 0.0001	
C-Time	0.090	1	0.090	63.76	< 0.0001	
AB	2.772×10^{-3}	1	2.772×10^{-3}	1.96	0.2040	
AC	0.015	1	0.015	10.95	0.0129	
BC	0.016	1	0.016	11.60	0.0114	
A^2	0.027	1	0.027	19.42	0.0031	
B^2	6.323×10^{-3}	1	6.323×10^{-3}	4.48	0.0722	
C^2	9.210×10^{-3}	1	9.210×10^{-3}	6.52	0.0379	
Residual	9.886×10^{-3}	7	1.412×10^{-3}			
Lack of Fit	9.886×10^{-3}	5	1.977×10^{-3}			
Pure Error	0.000	2	0.000			
Cor Total	2.71	16				
Fit Statistics	Std Dev =0.038		R^2= 0.9964			
	Mean =3.85		Adjusted R^2 = 0.9917			
	C.V. % 0.98		Predicted R^2 = 0.9695			
	Adeq Precision = 50.678					

J. Mex. Chem. Soc. **2024**, *68*(3)
Regular Issue

ISSN-e 2594-0317

Table 4. Initial ANOVA results and statistical parameters for response Y_2

Source	Sum of squares	df	Mean square	F-Value	p-Value Prob>F	Observation
Model	21.54	9	2.39	194.02	< 0.0001	**Significant**
A-Conc	3.40	1	3.40	275.38	< 0.0001	
B-Temp	16.85	1	16.85	1366.18	< 0.0001	
C-Time	0.047	1	0.047	3.81	0.0921	
AB	0.35	1	0.35	28.74	0.0011	
AC	4.069×10^{-4}	1	4.069×10^{-4}	0.033	0.8610	
BC	0.13	1	0.13	10.37	0.0146	
A^2	6.016×10^{-3}	1	6.016×10^{-3}	0.49	0.5075	
B^2	0.58	1	0.58	47.13	0.0002	
C^2	2.269×10^{-3}	1	2.269×10^{-3}	0.18	0.6809	
Residual	0.086	7	0.012			
Lack of Fit	0.086	5	0.017			
Pure Error	0.000	2	0.000			
Cor Total	21.63	16				
Fit Statistics	Std Dev =0.11		R^2= 0.9960			
	Mean =-1.66		Adjusted R^2 = 0.9909			
	C.V. % 6.68		Predicted R^2 = 0.9592			
	Adeq Precision = 47.301					

From the ANOVA (Tables 3 and 4), "F-value" of the model is 212.39 for inhibitory efficiency and 194.02 for corrosion rate respectively, implying that the models are significant. There is only a 0.01 % chance that the model could occur due to noise [30,42]. Probability values less than 0.05 indicate that the model terms are significant [34,43]. In the case of inhibitory efficacy, the factors A, B, C, the interactions AC, BC, and the quadratic effects A^2, C^2 are significant terms in the model. The P-value obtained for the interaction of type A B is 0.2040 (> 0.05). There is therefore no significant effect. Concerning the corrosion rate, the factors A, B, C, the interactions AB, B C, and the quadratic effect B^2 are significant terms in the model.

The regression analysis was examined in depth by evaluating the R^2, adjusted R^2, and predicted R^2 determination coefficients. R^2 indicates the proportion of total response variation predicted by the models. Correlation coefficients close to 1 indicate the adequacy of the models and the accuracy of the calculated constants [28]. Adjusted R^2 can be used to prevent probability errors, when a new term is added, and is a useful tool for comparing the explanatory power of models with different numbers of predictors. The predicted R^2 is used in regression analysis to indicate how well the model predicts responses for new observations. The predicted R^2 may be more useful than the adjusted R^2 for comparing models because it is calculated from observations not involved in the model estimation. The coefficients of determination R^2 and adjusted R^2 indicate

J. Mex. Chem. Soc. **2024**, *68*(3)
Regular Issue

ISSN-e 2594-0317

the quality of the polynomial fit and should be within about 0.20 of each other, to be in reasonable agreement. Both models have high coefficients of determination (R^2=0.9964 for inhibitory efficiency and R^2=0.9960 for corrosion rate. The adjusted R^2 value often decreases if statistically insignificant factors are added to the model. When R^2 and adjusted R^2 differ significantly, there is a strong chance that insignificant terms are included in the model [44], in our case the R^2 and adjusted R^2 coefficients are close to 1.00 for both models. Based on this study, for the first response (inhibitory efficacy), the predicted R^2 and adjusted R^2 values are 0.9695 and 0.9917, respectively, which suggests that the predicted and experimental inhibitory efficiencies are in perfect agreement. The R^2 equal to 0.9964 is in excellent accordance with the experimental results, which implies that this model can reveal 99.64 % of the variability. Furthermore, for the second response (corrosion rate), the values of R^2, predicted R^2 and adjusted R^2 are respectively 0.9960, 0.9592, and 0.9909 indicating a high correlation between the observed and predicted values. The coefficient of variation "CV" is the ratio of the standard error of the estimate to the mean value of the observed response and is a measure of the reproducibility of the model, generally a model can be considered reasonable if its CV is not greater than 15 % [45]. Thus, in this study, the obtained coefficient of variation value of 0.98 % (inhibitory efficiency) and 6.68 (corrosion rate) indicates a high precision and reliability of the experiments.

The ANOVA was then replicated after eliminating non-significant terms and the results for inhibitor efficacy and corrosion rate are given in Table 5 and Table 6. The adequacy of the regression models to interpret the experimental data at the 95% confidence level was examined using the ANOVA results. The significance of both main effects and interaction effects in the predictive models was assessed based on their probability values (p values). P-values less than 0.05 necessitated rejection of the null hypothesis suggesting that the particular term significantly affects the measured response of the system [40,41]. Finally, based on the final ANOVA for two responses Y1 and Y2, as well as the interactions with significant effects, a fitted regression model with statistical significance can be reported in the following equations:

$$Ln(Y_1) = 3.86 + 0.48A - 0.16B + 0.095C + 0.019AB - 0.044AC + 0.045BC - 0.085A^2 + 0.075C^2 \quad (6)$$

and:

$$Ln(Y_2) = -1.91 - 0.58A + 1.3B - 0.069C + 0.21AB + 0.13BC + 0.47B^2 \quad (7)$$

The normal probability plot of the residuals for the two responses (Y_1) and (Y_2) is depicted in Fig. 1**(a)** and 1**(b)**, respectively. The accuracy of the model should be estimated by the difference between the expected values and the actual values (residuals), which are expected to follow a normal distribution. The data in Fig. 1**(a)** and 1**(b)** should be evenly distributed and by a forty-five-degree line. The points are reasonably close to a straight line [46,47]. The straight lines obtained for the curves demonstrate that the studied residual follows a normal linear distribution, indicating that the models are appropriate for all examined responses.

Table 5. Final ANOVA results and statistical parameters for response Y_1.

Source	Sum of squares	df	Mean square	F-Value	p-Value Prob>F	Observation
Model	2.69	7	0.38	182.26	< 0.0001	**Significant**
A-Conc	2.30	1	2.30	1090.50	< 0.0001	
B-Temp	0.24	1	0.24	115.23	< 0.0001	
C-Time	0.090	1	0.090	42.70	< 0.0001	
AC	0.015	1	0.015	7.34	0.0241	
BC	0.016	1	0.016	7.77	0.0212	

J. Mex. Chem. Soc. **2024**, *68*(3)
Regular Issue

ISSN-e 2594-0317

Source	Sum of squares	df	Mean square	F-Value	p-Value Prob>F	Observation
A^2	0.022	1	0.022	10.30	0.0107	
C^2	0.017	1	0.017	8.11	0.0192	
Residual	0.019	9	2.109×10^{-3}			
Lack of Fit	0.019	7	2.712×10^{-3}			
Pure Error	0.000	2	0.000			
Cor Total	2.71	16				
Fit Statistics	Std Dev =0.046		R^2= 0.9930			
	Mean =3.85		Adjusted R^2 = 0.9875			
	C.V. % 1.19		Predicted R^2 = 0.9681			
	Adeq Precision = 46.367					

Table 6. Final ANOVA results and statistical parameters for response Y_2.

Source	Sum of squares	df	Mean square	F-Value	p-Value Prob>F	Observation
Model	21.53	6	3.59	362.58	< 0.0001	**Significant**
A-Conc	3.40	1	3.40	343.28	< 0.0001	
B-Temp	16.85	1	16.85	1703.00	< 0.0001	
C-Time	0.047	1	0.047	4.74	0.0544	
AB	0.35	1	0.35	35.83	0.0001	
BC	0.13	1	0.13	12.93	0.0049	
B^2	0.75	1	0.75	75.68	< 0.0001	
Residual	0.099	10	9.896×10^{-3}			
Lack of Fit	0.099	8	0.012			
Pure Error	0.000	2	0.000			
Cor Total	21.63	16				
Fit Statistics	Std Dev =0.099		R^2= 0.9954			
	Mean =-1.66		Adjusted R^2 = 0.9927			
	C.V. % 5.98		Predicted R^2 = 0.9838			
	Adeq Precision = 62.898					

J. Mex. Chem. Soc. **2024**, *68*(3)
Regular Issue

ISSN-e 2594-0317

An appropriate model can be determined based on the distribution of data points around the mean of the response variable as well. A uniformly distributed data point around the mean of the response variable suggests that the model is suitable (Fig. 2). Correlation between the predicted values of the response based on the model equation and the actual values obtained in the experiment were investigated using predicted versus actual plot. It can be seen that the proper correlation to the linear regression fit is obtained in this graph with an R^2 value of 0.9930 and 0.9954 for inhibitory efficacy and corrosion rate, which indicates that the model accurately describes the experimental data. Furthermore, the obtained measured values and their associated predicted values are compared in Table 7. The maximum error for

The plots of the residuals against predicted values for the final ANOVA in the case of the two responses examined are displayed in Fig. 3. From this Figure, it can be observed that there is not a considerable dispersion of the residuals for the two responses. Therefore, it appears that the proposed model was appropriate.

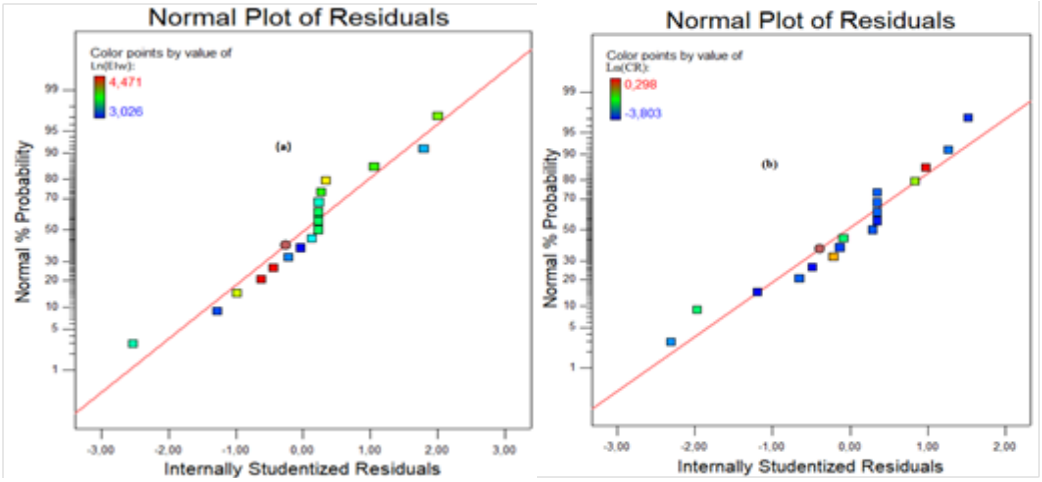

Fig. 1. Normal probability plot of the residuals for: **(a)** inhibitory efficiency and **(b)** corrosion rate.

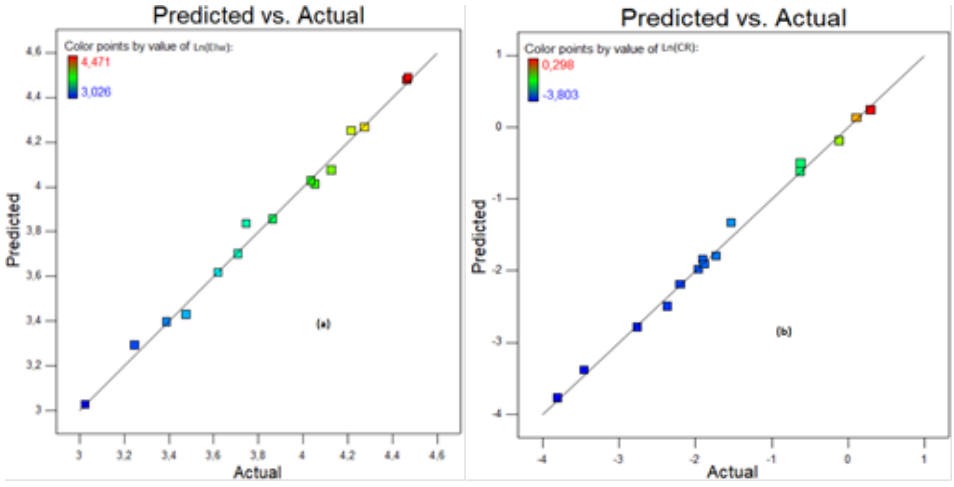

Fig. 2. Plots of predicted versus actual values for **(a)** inhibitory efficiency and **(b)** corrosion rate.

J. Mex. Chem. Soc. **2024**, *68*(3)
Regular Issue

ISSN-e 2594-0317

Table 7. Comparison between experimental and predicted values and calculation of residuals for the two responses (Y_1, Y_2)

Run	Response Y_1 (%) (%)		Response Y_2 (mg/cm².h)		Residue	
N°	$IE_{W(measured)}$	$IE_{W(predicted)}$	$CR_{(measured)}$	$CR_{(predicted)}$	e_i (IE_W)	e_i (CR)
1	86.88	87.38	0.0316	0.0339	-0.50	-0.0023
2	56.57	52.59	0.1412	0.1364	3.98	0.0048
3	32.36	30.72	0.1785	0.1649	1.64	0.0136
4	47.72	47.67	0.1523	0.1474	0.05	0.0049
5	29.64	30.41	1.3471	1.2308	-0.77	0.1163
6	42.40	43.20	0.1492	0.1593	-0.80	-0.0101
7	47.72	47.67	0.1523	0.1474	0.05	0.0049
8	67.77	69.65	0.0939	0.0815	-1.88	0.0124
9	47.72	47.67	0.1523	0.1474	0.05	0.0049
10	25.71	26.51	0.2163	0.2664	-0.80	-0.0501
11	62.01	59.44	0.5353	0.5206	2.57	0.0147
12	57.59	60.35	0.0636	0.0616	-2.76	0.0020
13	87.44	88.98	0.0223	0.0231	-1.54	-0.0008
14	37.33	36.67	0.1113	0.1121	0.66	-0.0008
15	40.82	45.33	0.8913	0.8006	-4.51	0.0907
16	71.90	73.79	0.538	0.5607	-1.89	-0.0227
17	20.61	20.90	1.1186	1.1429	-0.29	-0.0243

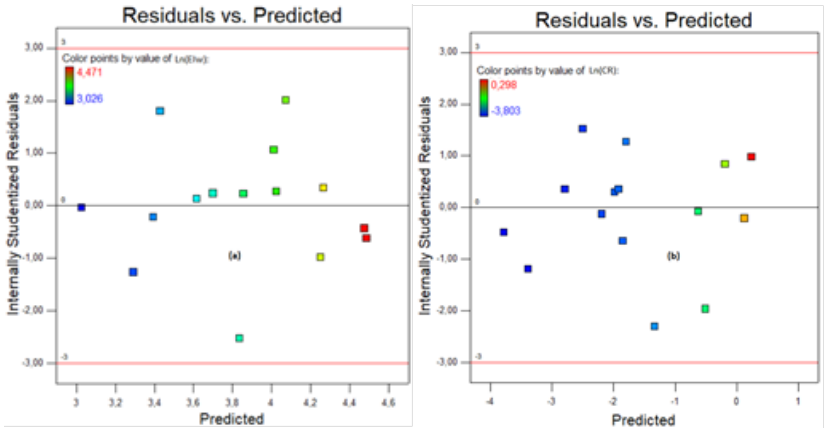

Fig. 3. Plot of the residual and predicted values of inhibition efficiency **(a)** and corrosion rate **(b)**.

J. Mex. Chem. Soc. **2024**, *68*(3)
Regular Issue

ISSN-e 2594-0317

Analysis of 3D response surfaces

3D response surfaces are plotted to enable viewing the simultaneous effects of two parameters on a response. Figures 3 and 4 display the response in terms of inhibition efficiency and corrosion rate respectively. Three combinations of interactions for every condition were statistically determined for each response. From the interactive effects of the extract concentration and temperature variables in Fig. 4**(a)** by keeping the immersion time at their constant value of 3 hours, we can observe that the inhibition efficiency of carbon steel decreases with an increase in temperature but increases with an increase in the concentration of the EBFL inhibitor. In general, corrosion inhibition depends on the adsorption of the organic inhibitor being used. The rate of desorption of EBFL molecules from the surface of carbon steel becomes more rapid at higher temperatures, which would be expected to be responsible for the decreased inhibition efficiency. Fig. 4**(b)** showed an interaction between the concentration of an inhibitor and the exposure time on the corrosion inhibition efficiency by maintaining the temperature at a value of 20 °C. The inhibition efficiency increases with both immersion time and increasing EBFL concentration. This Figure shows that the inhibition efficiency of the extract is quite good for an immersion period of 3 h for higher concentrations of EBFL. The interaction between immersion time and temperature shows that inhibition efficiency increases with increasing immersion time. The maximum inhibition efficiency is obtained at the highest immersion time and lowest temperature combination at the constant value of 800 ppm (Fig. 4**(c)**). This suggests faster adsorption and greater surface coverage on the carbon steel surface by EBFL at higher concentrations. Nevertheless, Fig. 5**(a)**, indicates that the corrosion rate decreases with the increase of the inhibitor concentration and also increases with an increase in the immersion time. Fig. 5**(b)** illustrates that the corrosion rate decreases with increasing inhibitor concentration and also increases with increasing time, as well as an increase in temperature leads to an increase in the corrosion rate as observed in Fig. 5**(c)** and decreases with increasing inhibitor concentration. This suggests physical adsorption.

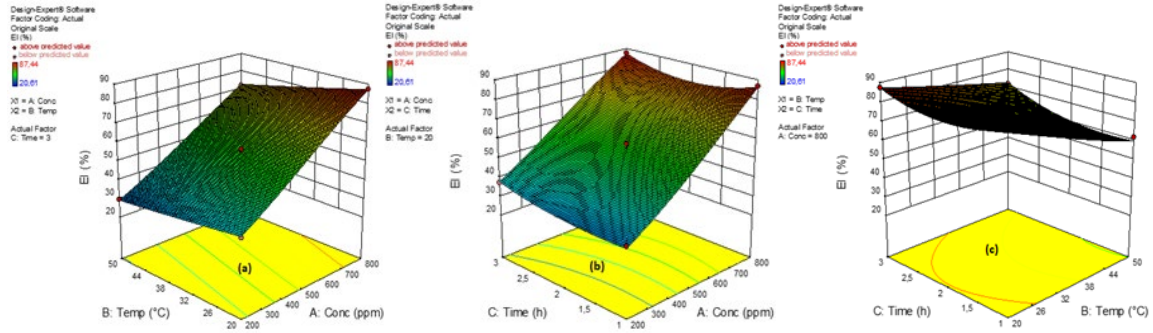

Fig. 4. 3D response surface diagrams for Inhibition Efficiency: **(a)** Temperature versus concentration, **(b)** Time versus concentration, and **(c)** Time versus temperature.

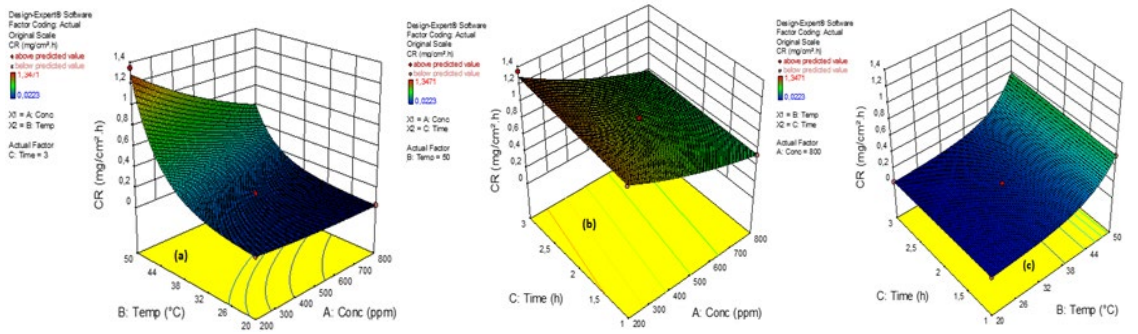

Fig. 5. 3D response surface diagrams for corrosion rate: **(a)** Temperature versus concentration, **(b)** Time versus concentration and **(c)** Time versus temperature.

J. Mex. Chem. Soc. **2024**, *68*(3)
Regular Issue

ISSN-e 2594-0317

Optimization and confirmation tests of the results

Response surface methodology (RSM) was used to choose the parameters that maximized the inhibition efficiency and corrosion rate of the butanolic extract (EBFL) as a corrosion inhibitor. The concentration of the inhibitor (A), temperature (B), and immersion time (C) were the three factors that were optimized. The predicted values of the responses are the optimal values based on the experimental findings shown in Table 7 and confirmed in Fig. 6, whose values of the optimal solution are close to 1 (or 100 %) for both examinations (Inhibition efficiency and corrosion rate). These values are picked as the parameter values that have the greatest impact on the response factor. According to Table 8, RSM tends to search, among a multitude of solutions, the top 10 best cases out of a large number of possibilities. The highest reported response values for corrosion rate and inhibition efficiency in this context are 0.02306 mg/cm^2•h and 88.9852 %, respectively.

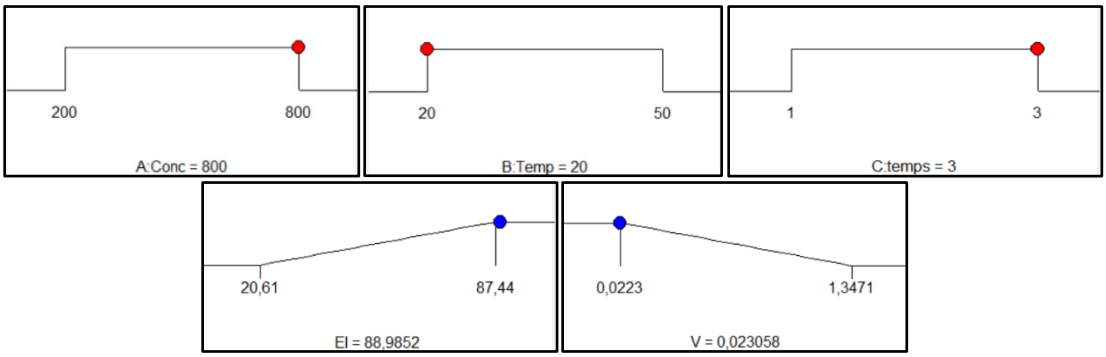

Fig. 6. Optimal conditions selected for parameters influence corrosion inhibition in the absence and presence of EBFL with their responses (inhibition efficiency and corrosion rate)

Table 8. Ten best solutions for parameters influencing corrosion inhibition in the absence and presence of EBFL, with their responses (inhibition efficiency and corrosion rate).

Number	Conc (ppm)	Temp (°C)	Time (h)	IEw (%)	CR (mg/cm².h)	Desirability
1	800.000	20.00	3.00	88.985	0.0231	1.00
2	799.795	20.026	2.984	88.744	0.0232	1.00
3	799.992	20.003	2.972	88.605	0.0232	1.00
4	797.143	20.000	2.999	88.744	0.0232	1.00
5	799.987	20.002	2.950	88.301	0.0233	1.00
6	799.960	20.002	2.941	88.186	0.0233	1.00
7	797.601	20.002	2.965	88.312	0.0234	1.00
8	798.887	20.002	2.930	87.360	0.0234	1.00
9	799.794	20.002	2.898	87.631	0.0235	1.00
10	786.274	20.001	2.999	87.875	0.0239	0.999

J. Mex. Chem. Soc. **2024**, *68*(3)
Regular Issue

ISSN-e 2594-0317

Calculation of the inhibitory efficiency and the corrosion rate at different temperatures from the models

To better understand the behavior of a metal in an aggressive medium and the nature of the metal/inhibitor interaction in this environment, it is interesting to determine the temperature values provided by the two suggested models in the range of 20 to 50 °C after 3 h of immersion. All the computations of the inhibitor efficiency and the corrosion rate, (Eqs. 6 and 7), were done using MATLAB software. From Table 9, we notice that EBFL has good inhibitory properties against the corrosion of carbon steel in 1M HCl medium. The increase in temperature leads to a decrease of the inhibitory efficiency showing a desorption phenomenon, i.e. the protective layer formed on the steel surface by adsorption of the extract is destroyed. According to [48, 49], this phenomenon was explained by the high sensitivity of the physical interactions of Van Der Waals type between the iron surface and the inhibitor. The inhibitory efficiency (IE_W) decreases while the corrosion rate (CR) increases with temperature in the range of 20 °C to 50 °C for all concentrations used. For all these concentrations, the corrosion rate (CR) also increases with temperature but takes lower values than the corrosion rate (CR) in the acid solution only.

Table 9. Calculation of the inhibitory efficiency and the corrosion rate from the two models proposed in the absence and presence of different concentrations of EBFL at different temperatures after 3h of immersion.

T(°C)	C(ppm)	$IE_{W_{calculated}}$(%)	$CR_{calculated}$(mg/cm²•h)
20	0	//	0.1903
	200	37.20	0.1121
	400	53.62	0.0661
	600	71.69	0.0389
	800	88.89	0.0229
30	0	//	0.2665
	200	34.55	0.1725
	400	49.80	0.1116
	600	66.59	0.0722
	800	82.57	0.0467
40	0	//	0.5453
	200	32.09	0.3874
	400	46.27	0.2753
	600	61.86	0.1956
	800	76.70	0.1390
50	0	//	1.6299
	200	29.82	1.2716
	400	42.97	0.9921
	600	57.96	0.7741
	800	71.24	0.6039

J. Mex. Chem. Soc. **2024**, *68*(3)
Regular Issue

ISSN-e 2594-0317

Adsorption mechanism

Adsorption parameters

The adsorption processes of inhibitors are governed by the chemical structure of the organic compounds, the nature and surface modification of the metal, the charge distribution in the molecule, and the type of aggressive medium [48]. Therefore, different isotherms including Langmuir, Temkin, Frumkin, and Freundlich, were checked to find the appropriate adsorption isotherm as listed in Table 10. The following relationship defines the value of the coverage rate (θ) of the metal surface by the adsorbed inhibitor:

$$\theta = \frac{IE_W}{100} \tag{8}$$

Table 10. The correlation coefficient of different adsorption isotherms at different temperatures.

Isotherms of dsorption	**Coefficient of correlation (R^2)**			
	20°C	**30°C**	**40°C**	**50°C**
Langmuir	0.9243	0.9242	0.9243	0.9243
Freundlich	0.9922	0.9922	0.9922	0.9922
Temkin	0.9556	0.9555	0.9556	0.9556
Frumkin	0.8119	0.7908	0.7382	0.6459

After having plotted the different isotherms at different temperatures, the most suitable correlation coefficient for use in our case is the Freundlich isotherm model in which the correlation coefficient of the curves is very close to the unit compared to the others (Fig. 7). From the Freundlich isotherm, we can easily deduce the adsorption constant reported in Table 11.

Thermodynamic parameters of adsorption

According to the Freundlich isotherm, (θ) is related to the inhibitor concentration ln C_{inh} by the following equation :

$$\log \theta = \log K_{ads} + a \log c \tag{9}$$

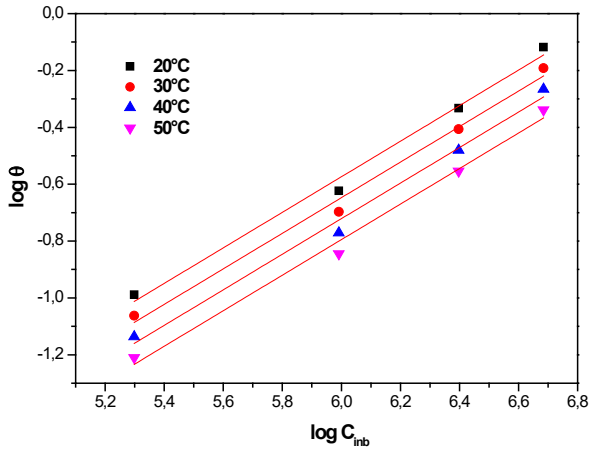

Fig. 7. Freundlich adsorption isotherm of carbon steel in 1M HCl in the presence of EBFL at different temperatures.

J. Mex. Chem. Soc. **2024**, *68*(3)
Regular Issue

ISSN-e 2594-0317

Table 11. Adsorption constants (K_{ads}) at different temperatures.

Plant	**Model Isothermal Freundlich**			
	Temperature (°C)	**Slope**	**Intercept**	**K_{ads}**
EBFL	20	0.62535	-4.32587	1.32×10^{-2}
	30	0.62533	-4.39951	1.23×10^{-2}
	40	0.62535	-4.47337	1.14×10^{-2}
	50	0.62528	-4.54670	1.06×10^{-2}

We note that the values of K_{ads} decrease with temperature. The equilibrium constant K_{ads} is related to the standard free energy of adsorption ΔG^0_{ads} by the following Eq.10 :

$$\Delta G^0_{ads} = -RT\, ln\left(C_{H_2O}\right)K_{ads} \tag{10}$$

where: $C_{H_2O} = 10^6\ mg\ /\ L$. R is the gas constant and T represents the absolute temperature. The standard enthalpy of adsorption ΔH^0_{ads} can also be deduced from the Vant'Hoff (Eq.11):

$$ln\left(K_{ads}\right) = -\frac{\Delta H_{ads}}{RT} + A \tag{11}$$

Fig. 8 exhibits the variation of ln(K_{ads}) versus 1/T. The slope gives ΔH^0_{ads}. Using the Gibbs Helmholtz equation to calculate the standard entropy of adsorption ΔS^0_{ads} from the Eq.12:

$$\Delta G^0_{ads} = \Delta H^0_{ads} - T\Delta S^0_{ads} \tag{12}$$

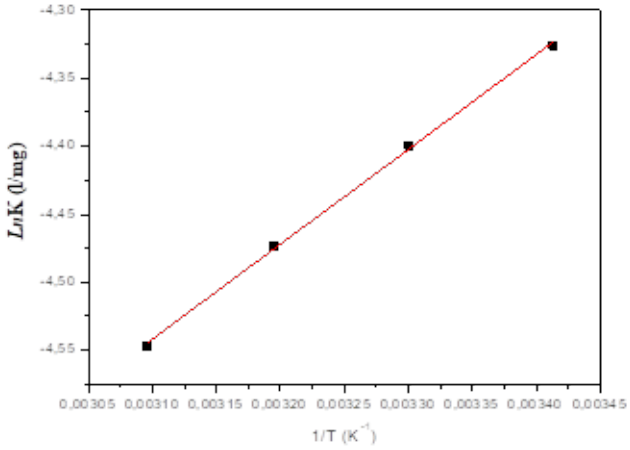

Fig. 8. The variation of ln (K_{ads}) as a function of inverse Temperature.

The thermodynamic data obtained for the EBFL are presented in Table 12.

J. Mex. Chem. Soc. **2024**, *68*(3)
Regular Issue

ISSN-e 2594-0317

Table 12. Thermodynamic parameters of EDFL in 1 M HCl medium for different temperatures.

EBFL Thermodynamic parameters				
T (K)	K_{ads}(mg/l)	ΔG^0_{ads}(kJ.mol^{-1})	ΔH^0_{ads}(kJ.mol^{-1})	ΔS^0_{ads}(J.mol^{-1}.K^{-1})
293	$1.32.10^{-2}$	-23.113		59.130
303	$1.23.10^{-2}$	-23.724	-5.788	59.195
313	$1.14.10^{-2}$	-24.309		59.173
323	$1.06.10^{-2}$	-24.890		59.139

From Table 12, under the same conditions, we see that the K_{ads} values of the EBFL decrease with increasing temperature. The negative values ΔG^0_{ads} indicate the spontaneity of the adsorption process and the stability of the adsorbed double layer on the metal surface. The obtained results of the adsorption ΔG_{ads} values close to −20 kJ/mol confirm the physisorption mechanism [20,49]. The enthalpy value calculated from the Vant'Hoff equation is of the order of -5.788 kJ/mol, which shows the exothermic character of the adsorption of the latter on the surface of the carbon steel confirming physisorption. This can also be explained by the decrease of the inhibitory efficiency by increasing the temperature. We note that ΔS^0_{ads} in the presence of EBFL is positive. This involves an increase in the disorder that accompanies the adsorption of inhibitory molecules from the solution onto the metal surface [50].

Determination of activation energies

In this study, the Arrhenius-type dependence observed between the corrosion rate and temperature is represented by the following relationship [51]:

$$ln\,CR = ln\,A - \frac{Ea}{RT} \tag{13}$$

where A is a constant (pre-exponential factor), Ea is the activation energy, R is the universal gas constant and T is the absolute temperature. A plot of the logarithm of the CR versus 1/T showed a straight line. As exhibited in Fig. 9, the values of apparent activation energy E_a were obtained from the slope ($-E_a/R$).

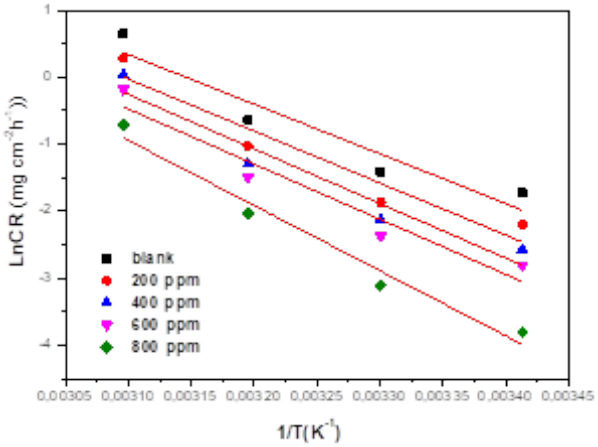

Fig. 9. Arrhenius diagram of the corrosion rates of carbon steel in 1 M HCl medium in the absence and presence of the different concentrations of EBFL.

J. Mex. Chem. Soc. **2024**, *68*(3)
Regular Issue

ISSN-e 2594-0317

The alternative formulation of the Arrhenius relation as expressed in Equation 14 was used to determine the activation enthalpy ΔH_a and activation entropy ΔS_a values [20,49,52].

$$ln CR = \left[ln \frac{RT}{Nh} + \frac{\Delta S_a}{RT} \right] - \frac{\Delta Ha}{RT} \quad (14)$$

where, h represents the Planck's constant (6.626×10^{-34} J.s) and N is the Avogadro's number ($6{,}022\times10^{23}$ mol^{-1}). The plot of ln (CR/T) versus (1/T) showed a straight line (Fig. 10). The values of ΔH_a and ΔS_a were deduced from the slope ($-\Delta H_a/R$) and intercept ($\ln(RT/Nh)+ \Delta S_a/R$).

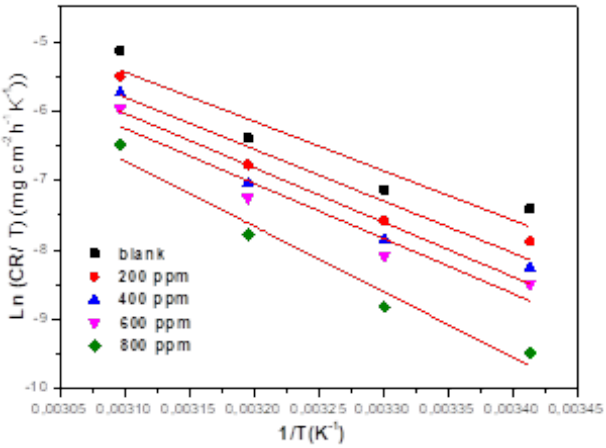

Fig. 10. Alternative Arrhenius diagram of the corrosion rates of carbon steel in 1M HCl medium in the absence and presence of the different concentrations of EBFL.

Table 13. Activation parameters of X2C30 carbon steel in 1M HCl in the absence and presence of different concentrations of EBFL.

EBFL (ppm)	E_a(kj•mol $^{-1}$)	ΔH_a^0(kj•mol^{-1})	ΔS_a^0(J•mol^{-1})
blank	55.906	53.350	95.606
200	63.266	60.710	116.305
400	70.610	68.054	136.949
600	78.001	75.445	157.744
800	85.381	82.825	178.505

The findings achieved in this study reveal that the values of (E_a) ranged from 63.266 to 85.381 kJ mol^{-1}. It is obvious that the apparent activation energy (E_a) increased with the concentration of EBFL and was more than in the absence of an inhibitor as displayed in Table 13. This increase reflects that the inhibitory molecules of EBFL are physisorbed [52-55]. We note that the change in the values of E_a may be attributed to the geometric blocking effect of adsorbed inhibitive species on the steel surface. The positive sign of the enthalpy values of activation, thus expressing its difficult course, reveals the endothermic nature of the carbon steel dissolution process.

J. Mex. Chem. Soc. **2024**, *68*(3)
Regular Issue

ISSN-e 2594-0317

Morphological characterization

SEM analysis is a useful tool to characterize the surface morphology of carbon steel samples. Fig. 11**(a)**, 11**(b)**, and 11**(c)**, displayed the surface morphology of carbon steel samples immersed in 1 M HCl solution without and with the addition of 800 ppm of EBFL for 3 h at 293 K. Fig. 11**(a)** shows the polished lines on the surface of carbon steel before its exposure to the testing environments. Fig. 11**(b)** show that the surface of the sample is heavily damaged and severely corroded compared However, in the presence of 800ppm of the inhibitor EBFL as shown in Fig. 11**(c)**, the external morphology appears softer, indicating a protected surface. These results support all obtained results cited above.

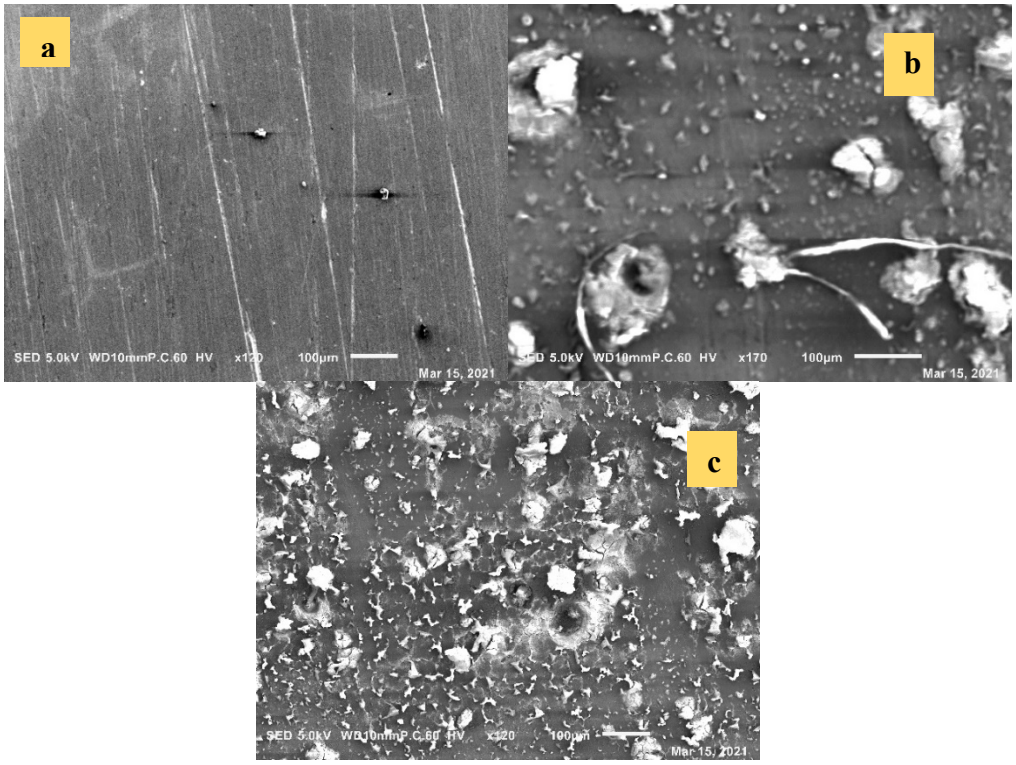

Fig. 11. SEM pictures of carbon steel before corrosion **(a)** in acid solution **(b)** and **(c)** in the presence of 800ppm after 3 h immersion time at 293 K.

Conclusions

In this work, a Response Surface Methodology (RSM) based on the Composite Centered Design (CCD) was used to study and statistically analyze the effect of the extract (EBFL) on the corrosion inhibition of carbon steel (X2C30), in a 1M HCl acid medium. This statistical method allows the establishment of mathematical models involving different parameters that influence the inhibitory efficiency as well as the corrosion rate, namely: the inhibitor concentration, the immersion time, and the temperature. The weight loss method was employed to evaluate and analyze the inhibitory effect and the influence of specific parameters on the corrosion of the carbon steel electrode.

The different results obtained from this investigation are:

- Quadratic logarithmic models modeled the inhibitory efficiency and corrosion rate as responses. From the statistical analysis ANOVA we confirmed that both obtained models are significant (P=0.0001< 0.05) with a satisfactory correlation between the measured values and those adjusted (R^2 =99.30 % and R^2ajus= 98.75 %) for the case of inhibitory efficiency and (R^2 =99.54 % and R^2ajus= 99.27 %) for

J. Mex. Chem. Soc. **2024**, *68*(3)
Regular Issue

ISSN-e 2594-0317

the corrosion rate. According to the experimental results obtained with the highest desirability, the highest response values reported for the corrosion rate and inhibition efficiency in this context were 0.02306 mg/cm^2•h and 88.9852 % respectively.

- The study of the influence of concentration and temperature on the inhibitory efficiency and the corrosion rate was carried out to confirm the adsorption model on the metal surface. Several factors highlighted the physisorption nature of the EBFL adsorption namely: the apparent activation energy of the steel dissolution process, which is higher than the activation energy value, obtained in the case of the acid alone, the negative values of the free energy of adsorption as well as the negative value of the enthalpy of adsorption. The thermodynamic study showed that the adsorption of the extract on the steel surface is spontaneous and follows the Freundlich adsorption isotherm model. SEM micrographs confirmed the adsorption of protective film on carbon steel.

Acknowledgements

The authors like to thank the Algerian General Direction of Research (*DGRSDT*) for their support.

References

1. Al-Moubaraki, A.H.; Obot, I.B. *J. Saudi Chem. Soc.* **2021**, *25*, 101370. DOI: https://doi.org/10.1016/j.jscs.2021.101370.
2. Al-Janabi, Y.T. in: *Corrosion Inhibitors in the Oil and Gas Industry*, Wiley-VCH Verlag GmbH & Co. KgaA, **2020**. DOI: https://doi.org/10.1002/9783527822140.ch1.
3. Trabanelli, G. *Corrosion.* **1991**, *47*, 410-419. DOI: https://doi.org/10.5006/1.3585271.
4. Liu, J.; Yu, W.; Zhang, J.; Hu,S.; You, L.; Qiao, G. *Appl. Surf. Sci.* **2010**, *256*, 4729- 4733. DOI: https://doi.org/10.1016/j.apsusc.2010.02.082.
5. Rice, J. *Mechanics of Solids*. Encyclopedia Britannica, 1993.
6. Musa, A.Y.; Khadom, A.A.; Kadhum, A.A.H.; Mohamad , A.B; Takriff, M.S. *J. Taiwan Inst. Chem. Eng.* **2010**, *41*, 126-128. DOI: https://doi.org/10.1016/j.jtice.2009.08.002.
7. Ameer, M.A. ; Fekry, A.M. *Int. J. Hydrogen Energy.* **2010**, *35*, 11387-11396. DOI: https://doi.org/10.1016/j.ijhydene.2010.07.071.
8. Khaled, K.F. *Mater. Chem. Phys.* **2011**, *125*, 427-433. 542. DOI: https://doi.org/10.1016/j.matchemphys.2010.10.037.
9. Balulescu, M.; Herdan, J. *J. Synth. Lubr.* **1997**, *14*, 35-45. 544. DOI: https://doi.org/10.1002/jsl.3000140104.
10. Zakeri, A. ; Bahmani, E.; Rouh Aghdam, A.S. *Corros. Commun.* **2022**, *5*, 25-38. DOI: https://doi.org/10.1016/j.corcom.2022.03.002.
11. Yaro, A.S. ; Al-Jendeel, H. ; Khadom, A.A. Desalination. **2011**, *270*, 193-198. DOI: https://doi.org/10.1016/j.desal.2010.11.045.
12. Hussin, M.H. ; Kassim, M.J. Mater. Chem. Phys. **2011**, *125*, 461-468. DOI: https://doi.org/10.1016/j.matchemphys.2010.10.032.
13. Valek, L.; Martinez, S. *Materials Letters*. **2007**, *61*, 148-151. DOI: https://doi.org/10.1016/j.matlet.2006.04.024.
14. Behpour, M.. Ghoreishi, S.M. ; Khayatkashani , M.; Soltani ,N. *Mater. Chem. Phys.* **2012**, *131*, 621-633. DOI: https://doi.org/10.1016/j.matchemphys.2011.10.027.
15. Soltani, N.; Tavakkoli, N.; Kashani, M.K.; Mosavizadeh, A.; Oguzie, E.E.; Jalali, M.R. *J. Ind. Eng. Chem.* **2014**, *20*, 3217-3227. DOI: https://doi.org/10.1016/j.jiec.2013.12.002.

J. Mex. Chem. Soc. **2024**, *68*(3)
Regular Issue

ISSN-e 2594-0317

16. Dehghani, A.; Bahlakeh, G.; Ramezanzadeh, B.; Ramezanzadeh, M. *J. Ind. Eng. Chem*. **2020**, *84*, 52-71. DOI: https://doi.org/10.1016/j.jiec.2019.12.019.
17. Fadhil, A.A.; Khadom, A.A.; Ahmed, S.K.; Liu, H.; Fu, C.; Mahood,H.B. *Surf. Interfaces.* **2020**, *20*, 100595. DOI:https://doi.org/10.1016/j.surfin.2020.100595.
18. Wang, Q.; Tan,B.; Bao, H.; Xie , Y; Mou, Y.; Li, P.; Chen, D.; Shi ,Y.; Li, X.; Yang, W. *Bioelectrochemistry*. **2019**, *128*, 49-55. DOI: https://doi.org/10.1016/j.bioelechem.2019.03.001.
19. Chaubey, N.; Singh, V.K.; Savita ; Quraishi, M.A.; Ebenso, E.E. *Int. J. Electrochem. Sci.* **2015**, *10*, 504-518. DOI: https://doi.org/10.1016/S1452-3981(23)05009-5.
20. Boukhedena, W. ; Deghboudj, S. ; Benahmed, M. ; Laouer, H. *J. Mex. Chem. Soc*. **2022**, *66*, 248-271. DOI: http://dx.doi.org/10.29356/jmcs.v66i2.1630.
21. Kalla, A. ; Benahmed, M. ; Djeddi,N. ; Akkal,S.; Laouer, H. *Int J Ind Chem*. **2016**,*7*, 419-429. DOI: https://doi.org/10.1007/s40090-016-0094-8.
22. Anwar, B.; Khairunnisa, T. ; Sunarya, Y. *Int. J. Corros. Scale Inhib.* **2020**, *9*, 244-256.
23. Oguzie, E.E. *Corros. Sci.* **2007**,*49*, 1527-1539. DOI: https://doi.org/10.1016/j.corsci.2006.08.009.
24. M'hiri, N.; Veys-Renaux, D.; Rocca, E.; Ioannou, I.; Boudhrioua,N.M.; Ghoul,M. *Corros. Sci.* **2016**, *102*, 55-62. DOI: https://doi.org/10.1016/j.corsci.2015.09.017.
25. Kosari, A.; Davoodi, A.; Moayed; M.H.; Gheshlaghi, R. *Corros.* **2015**, *71*, 819-827. DOI: https://doi.org/10.5006/1578.
26. Haris, N.I.N.; Sobri, S.; Kassim, N. *Mater. Corros.* **2019**,*70*, 1111-1119. DOI: https://doi.org/10.1002/maco.201810653.
27. Okewale, A.; Adesina, O.; Akpeji, B. *Nig. J. Basic Appl. Sci.* **2019**, *27*, 47-56. DOI: https://doi.org/10.4314/njbas.v27i2.7.
28. Caglar, A., Sahan , T.; Selim Cogenli, M.; Yurtcan, A.B.; Aktas, N.; Kivrak, H. *Int. J. Hydrogen Energy*. **2018**, *43*, 11002-11011. DOI: https://doi.org/10.1016/j.ijhydene.2018.04.208.
29. Im, J.-K.; Cho,I.-H; Kim,S.-K.; Zoh, K.-D. *Desal.* **2012**, *285*, 306-314. DOI: https://doi.org/10.1016/j.desal.2011.10.018.
30. Liu, Y.; Wang , J.; Zheng ,Y.; Wang, A. *Chem. Eng. J.* **2012**, *184*, 248-255. DOI: https://doi.org/10.1016/j.cej.2012.01.049.
31. Akkal, S.; Louaar, S.; Benahmed, M.; Laouer, H.; Duddeck, H. *Chem. Nat. Compd.* **2010**, 46, 719-721. DOI: https://doi.org/10.1007/s10600-010-9724-0.
32. Obi-Egbedi, N.O.; Essien, K.E.; Obot, I.B.; Ebenso, E.E. *Int. J. Electrochem. Sci.* **2011**, *6*, 913-930. DOI: https://doi.org/10.1016/S1452-3981(23)15045-0.
33. Tinsson, W. in: *Plans d'expérience: constructions et analyses statistiques*. Springer Science & Business Media, **2010**.
34. Mongomery, D. in: *Montgomery: design and analysis of experiments*. John Willy & Sons, **2017**.
35. Ladurée, D.; Paquer, D.; Rioult, P. *Rec. Trav. Chim. Pays-Bas.* **1977**, *96*, 254-258. DOI: https://doi.org/10.1002/recl.19770961004.
36. Obot, I. ; Obi-Egbedi, N. *Curr. Appl. Phys,* **2011**, *11*, 382-392.DOI: https://doi.org/10.1016/j.cap.2010.08.007.
37. Abdallah, M. *Corros. Sci.* **2002**, *44*, 717-728. DOI: https://doi.org/10.1016/S0010-938X(01)00100-7.
38. Ali, S.A.; El-Shareef, A.M. ; Al-Ghamdi , R.F. ; Saeed, M.T. *Corros. Sci.* **2005**, *47*, 2659-2678. DOI: https://doi.org/10.1016/j.corsci.2004.11.007.
39. Lawson, J. in: *Design and Analysis of Experiments with SAS*. Chapman and Hall/CRC, New York, **2010**.
40. Yaghoobi, H.; Fereidoon, A. *Polym. Compos.* **2018**, *39*, E463-E479. DOI: https://doi.org/10.1002/pc.24596.
41. Yaghoobi, H.; Fereidoon, A. *J. Nat. Fibers*. **2019**, *16*, 987-1005. DOI: https://doi.org/10.1080/15440478.2018.1447416.

J. Mex. Chem. Soc. **2024**, *68*(3)
Regular Issue

ISSN-e 2594-0317

42. Cobas, M.; Sanromán, M.A.; Pazos, M. *Bioresour. Technol.* **2014,** *160*, 166-174. DOI: https://doi.org/10.1016/j.biortech.2013.12.125.
43. Yazici, E.Y.; Deveci, H. *Hydrometallurgy*. **2013**, *139*, 30-38. DOI: https://doi.org/10.1016/j.hydromet.2013.06.018.
44. Hicks,C.R. in: *Fundamental concepts in the design of experiments*. Holt, Rinehart and Winston, New York, **1964**.
45. Rossi, R.J. in: *Applied biostatistics for the health sciences*. John Wiley & Sons, **2022**.
46. Garba, Z.N.; Bello, I.; Galadima, A.; Lawal , A.Y. *KIJMS.* **2016**, *2*, 20-28. DOI: https://doi.org/10.1016/j.kijoms.2015.12.002.
47. Anadebe, V.C.; Onukwuli, O.D. ; Omotioma, M.; Okafor, N.A. *Mat. Chem. Phys.* **2019**, *233*, 120-132. DOI: https://doi.org/10.1016/j.matchemphys.2019.05.033.
48. Ahamad, I.; Prasad, R. ; Quraishi, M. *Corros. Sci.* **2010**, *52*, 933-942. DOI: https://doi.org/10.1016/j.corsci.2009.11.016.
49. Boukhedena, W.; Deghboudj, S. *J. Electrochem. Sci. Eng*. **2021**, *11*, 227-239. DOI: https://doi.org/10.5599/jese.1050.
50. Wang, H.-L.; Fan, H.-B.; Zheng, J.-S. *Mat. Chem. Phys.* **2003**, *77*, 655-661. DOI: https://doi.org/10.1016/S0254-0584(02)00123-2.
51. Huang, W. ; Zhao, J. *Colloids Surf. A*. **2006**, *278*, 246-251. DOI:https://doi.org/10.1016/j.colsurfa.2005.12.028.
52. Fiala, A.; Boukhedena, W.; Lemallem, S.E.; Brahim Ladouani, H.; Allal, H. *J. Bio- Tribo-Corros*. **2019**, *5*, 1-17. DOI: https://doi.org/10.1007/s40735-019-0237-5.
53. Kosari, A.; Momeni, M.; Parvizi, R.; Zakeri, M.; Moayed, M.H.; Davoodi, A.; Eshghi, H. *Corros. Sci.* **2011**, *53*, 3058-3067. DOI: https://doi.org/10.1016/j.corsci.2011.05.009.
54. Umoren, S.A; Obot, I.B. *Surf. Rev. Lett.* **2008**, *15*, 277-286. DOI: https://doi.org/10.1142/S0218625X08011366.
55. Ebenso, E.E. *Mat. Chem. Phys.* **2003**, *79*, 58-70. DOI: https://doi.org/10.1016/S0254-0584(02)00446-7.